U.D.C. 541.13

Thin-layer Electrochemistry

R.S.Tyurin, Yu.S.Lyalikov, and S.I.Zhdanov

This review deals with the theoretical foundations of the methods of thin-layer electrochemistry (chronopotentiometry, voltammetry, and the steady-state current method), and with the application of these methods to the measurement of rate constants of electrochemical reactions, to the study of adsorption, and to the determination of diffusion coefficients, number of electrons involved in the reaction, etc. The scope of the methods of thin-layer electrochemistry, and their advantages in specific cases over alternative methods of studying electrode processes, are discussed. 53 references.

CONTENTS

I. Introduction	1086
II. Theory of thin-layer electrochemistry	1086
1. Chronopotentiometry	1087
2. Voltammetry	1090
3. Steady-state current method	1095
III. Special features and scope of thin-layer electrochemistry	1098
1. Edge effect	1098
2. Influence of lack of parallelism and of surface roughness of the working electrode	1098
3. Scope and advantages of the methods of thin-layer electrochemistry	1099
IV. Practical applications of thin-layer electrochemistry	1099

I. INTRODUCTION

The most important recent advances in electrochemistry have been concerned with the development of the theory of electrode processes, which is relevant not only to electrochemistry itself but also to related branches of science and technology. Electrochemical concepts and techniques are used, for example, in studies of biological processes, in studies of the electrochemical and adsorption properties of the semiconductor–electrolyte interface, etc.

Electrochemical processes often need to be studied not only on macroscopic samples but also on small (and even very small) samples. Measurements with small volumes of solution have long been carried out in polarography with the dropping mercury electrode, but the smallest practical volume of solution in cells of conventional design has been 0.2–0.3 ml. The first papers on thin-layer electrochemistry appeared in the early 1960's, and laid the foundations for the solution of the theoretical and the practical problems inherent in studies of the electrolysis of solutions held in a narrow gap between two electrodes. During the last decade there have been significant developments in this area of electrochemistry. Depending on the method used to display the infromation, we can classify this work into thin-layer chronopotentiometry, oscillographic voltammetry, and the steady-state current method. The methods of thin-layer electrochemistry have some definite advantages over the corresponding methods which rely on large volumes of solution. These advantages stem from the fact that the convective transfer of electrochemically active material is practically negligible in thin layers of electrolyte, and therefore the mathematical description of the electrode processes is greatly simplified. Hence, important kinetic parameters such as the rate constants k, the diffusion coefficients D, and the number of electrons n can be evaluated without difficulty. Thin-layer methods using solution volumes as small as 10^{-3} ml are also convenient for the analysis of strongly radioactive solutions which cannot be safely handled in large volumes. Insufficient attention has been paid to thin-layer electrochemistry in the Soviet literature: this review aims to rectify the omission in some measure.

II. THEORY OF THIN-LAYER ELECTROCHEMISTRY

We shall discuss the theory of thin-layer electrochemistry by considering the electrode processes in a thin cylindrical layer of solution of thickness l held between two plane-parallel coaxial electrodes of area A and radius r. The thickness of the layer can be controlled, for example, by using a micrometer as shown in Fig. 1. The volume of solution between the electrodes is $lA \simeq 10^{-3}$ ml. In order to monitor the electrode potential, the experimental solution can be held in contact with a large volume of the same solution through the cylindrical face of the thin layer (of area $2\pi rl$).

Fig. 2 shows the circuit diagram for a thin-layer cell consisting of a pair of plane-parallel electrodes, an auxiliary electrode, and a standard electrode, with suitable connections. Several methods of connection can be used. If the potentials of the working electrodes W_1 and W_2 are controlled independently by means of a standard and an auxiliary electrode, as shown in Fig. 2, we have a coupled thin-layer cell. If the electrode potentials E_1 and E_2 are equal, the cell has effectively one working electrode of total area $2A$ and solution thickness $l/2$. If one of the electrodes is left open-circuited, it acts as an inert plate. Lastly, if the standard and the auxiliary electrode are omitted we have a simple two-electrode thin-layer cell.

As an alternative to the plane-parallel electrodes[1–4], the electrodes for thin-layer electrochemical cells can be in the form of thin wires in a narrow glass or plastic tube[5,6]. A cell of this type is shown in Fig. 3. The thickness of the layer of solution can be varied by suitable choice of wire diameter and channel bore. The electrode

material can be graphite, platinum, mercury, or other metals; for combined electrochemical and spectrophotometric measurements glass plates coated with a conducting layer have been used [1,7-11].

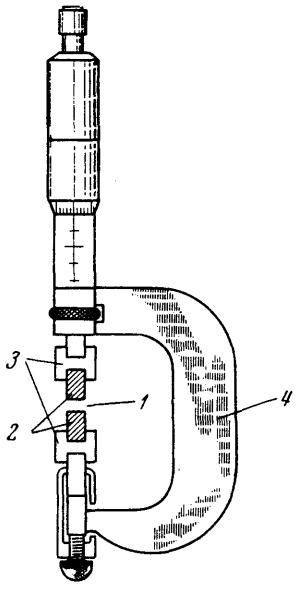


Figure 1. Plane-parallel micrometric electrodes: *1*) gap, *2*) platinum electrodes, *3*) insulating collars, *4*) micrometer.

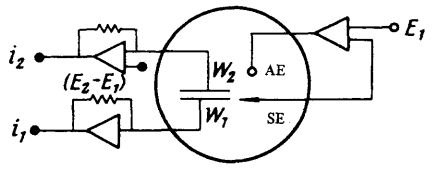


Figure 2. Circuit diagram of a two-electrode thin-layer cell: W_1 and W_2 are the working electrodes, AE is the auxiliary electrode, SE is the standard electrode.

1. Chronopotentiometry

We shall consider a solution containing an electrochemically active material in a thin-layer cell, confined between the boundaries 0 and l, so that $0 < x < l$. Only one of the two close-spaced electrodes is working, and the second electrode behaves as the wall of the cell.

If the material O is reduced at a constant current density i (galvanostatic conditions), and if the edge effect can be neglected†, the concentration of O at the electrode at any instant $c_O(0, t)$ can be calculated by the Laplace transform [12].

†See p. 1098.

Christensen and Anson [2] have shown that

$$c_O(0,t) = c_O^0 - \frac{il}{nFAD}\left[\frac{Dt}{l^2} + \frac{1}{3} - \frac{2}{\pi^2}\sum_{k=1}^{\infty}\frac{1}{k^2}\exp\left(-\frac{\pi^2 k^2 Dt}{l^2}\right)\right] \quad (1)$$

where c_O^0 is the initial concentration of O.

For large l, Eqn. (1) reduces to the familiar chronopotentiometric equation.

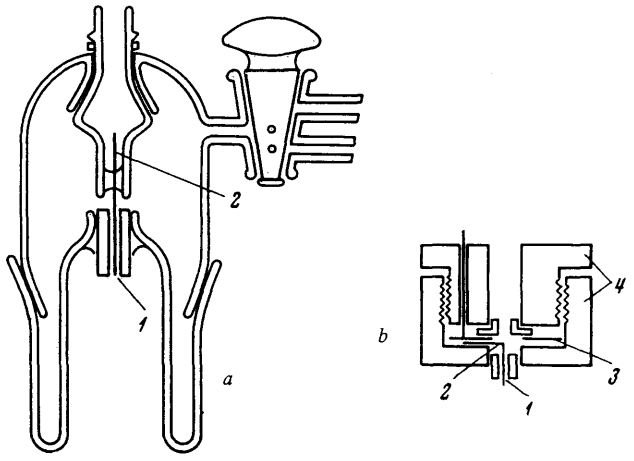


Figure 3. Types of capillary-filament electrode: *1*) gap, *2*) working electrode, *3*) Pt contact disk, *4*) Teflon body.

The time for complete removal of the depolariser from the layer adjacent to the electrode, when $c_O(0, t) = 0$, is called the transient time τ.

If τ is so large that $l^2 < \tau D$, the exponential terms in Eqn. (1) can be ignored, and the following expression for τ is obtained:

$$\tau = \frac{nFAlc_O^0}{i} - \frac{l^2}{3D}. \quad (2)$$

If the Nernst equation applies, the variation of potential with time $[E = f(t)]$ for the reversible redox couple O–R is given by the expression

$$E = E^0 + \frac{RT}{nF}\ln\frac{\tau - t + \frac{2l^2}{\pi^2 D}\sum_{k=1}^{\infty}\frac{1}{k^2}\exp\left(-\frac{\pi^2 k^2 Dt}{l^2}\right)}{t + \frac{l^2}{3D} - \frac{2l^2}{\pi^2 D}\sum_{k=1}^{\infty}\frac{1}{k^2}\exp\left(-\frac{\pi^2 k^2 Dt}{l^2}\right)} \quad (3)$$

where E^0 is the normal potential of the couple O–R. Eqn. (3) assumes equality of the diffusion coefficients of the oxidised and the reduced form of the material. The quantity $l^2/3D$ and the exponential terms of Eqn. (3) can be made small in comparison with t. In this case $E = E^0$ at $t = \tau/2$. The second term in the right-hand side of Eqn. (2) can be ignored when l is small and the concentration of O in solution is large enough. Thus, for $l = 10^{-3}$ cm and $D = 10^{-5}$ cm^2 s^{-1}, we have $l^2/3D \simeq 3 \times 10^{-2}$ s, and the second term in Eqn. (2) can be neglected under these

conditions if $\tau > 3$ s. Eqn. (3) then reduces to Faraday's law in the form used in constant-current coulometry:

$$\tau = \frac{nFAlc_0}{i} \qquad (4)$$

or

$$Q = nFAlc_0 . \qquad (5)$$

(*a*) Determination of the number of electrons in the reaction

Eqn. (4) can be used to evaluate n when the diffusion coefficients of the species being studied are not known. The cell used for this purpose has very closely spaced electrodes, to make $l^2/3D$ much smaller than the transient time. Thin-layer chronopotentiometry has been used to determine the number of electrons involved in the oxidation of *N,N*-dimethyl-*p*-phenylenediamine. The reaction goes through the steps

$$H_2N{-}C_6H_4{-}N(CH_3)_2 - e \rightleftarrows [H_2N{-}C_6H_4{-}N(CH_3)_2]^+ ,$$

$$[H_2N{-}C_6H_4{-}N(CH_3)_2]^+ - e \rightleftarrows NH{=}C_6H_4{=}N(CH_3)_2^+ + H^+ .$$

Conventional chronopotentiometric measurements [13] on platinum electrodes in acid solutions indicate a two-electron transition, but the interpretation of the results is complicated by subsequent chemical changes of the reaction products. The mean of the experimental values ($n = 1.97$) obtained in thin-layer experiments is in very good agreement with the value ($n = 2$) proposed for the oxidation of *N,N*-dimethyl-*p*-phenylenediamine to the di-imine. The thin-layer experiment gives more accurate values than conventional controlled-potential electrolysis [2,14]. Sharper chronopotentiograms are obtained in the thin-layer cell than in a conventional cell, as shown by the curves in Fig. 4 for the oxidation of *p*-phenylenediamine.

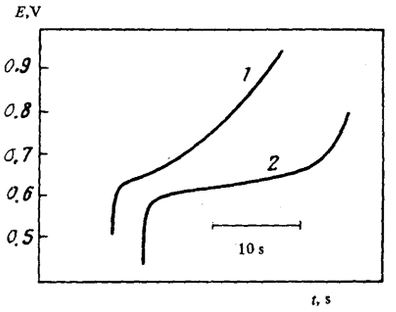


Figure 4. Chronopotentiograms for the oxidation of *p*-phenylenediamine: *1*) diffusion cell ($c = 4.72$ mM, current density 0.6 μA cm^{-2}); *2*) thin-layer cell ($c = 4.99$ mM, current density 0.09 μA cm^{-2}). In both cases the supporting electrolyte is 1 M H_2SO_4.

This is because a sharp transition to the next reaction (for example, the oxidation of water) sets in as soon as the whole of the material in the thin layer between the electrodes has been oxidised. In contrast, a significant fraction of the current in diffusion chronopotentiometry is carried by the oxidation of the experimental material which diffuses from the more remote layers of solution when the layer adjacent to the electrode has been depleted: as a result, the potential changes more gradually with time.

(*b*) Determination of diffusion coefficients

Oglesby and coworkers [15] have shown, by analysing Eqn. (2), that the diffusion coefficient of the experimental material can be determined even if the concentration of the solution and the surface area of the working electrode are not known. Thus, a plot of τ against $1/i$ is a straight line whose intercept on the τ axis gives $-l^2/3D$ (Fig. 5).

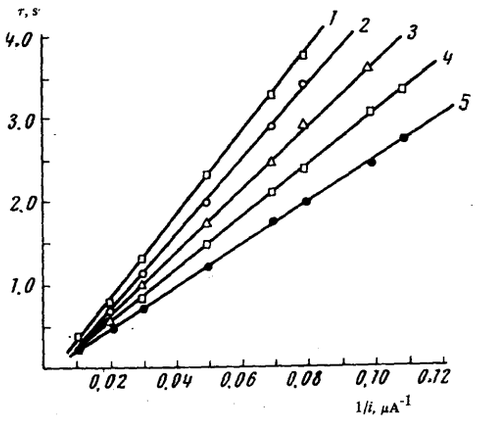


Figure 5. Plots of τ against $1/i$ for different thicknesses of solution: *1*) 1.88×10^{-3}, *2*) 1.62×10^{-3}, *3*) 1.37×10^{-3}, *4*) 1.12×10^{-3}, *5*) 0.864×10^{-3} cm. Area of working electrode 0.27 cm^2. Experimental solution $K_3Fe(CN)_6$ in 0.5 M Na_2SO_4.

Knowing l, the diffusion coefficient of the electrochemically active species can be calculated. Table 1 shows the diffusion coefficients for $Fe(CN)_6^{3-}$ in 0.5 M Na_2SO_4 obtained for different values of the layer thickness l.

Table 1. Diffusion coefficient of $Fe(CN)_6^{3-}$ in 0.5 M Na_2SO_4.

$10^3 l$, cm	$l^{2/3}D$, s	$10^5 D$, cm^2 s^{-1}
0.864	0.0502	0.49
1.12	0.0883	0.47
1.37	0.140	0.45
1.62	0.236	0.37
1.88	0.252	0.47

Average $D = 0.45 \times 10^{-5}$ cm^2 s^{-1}

(*c*) Determination of the rate constants of chemical reactions

Thin-layer chronopotentiometry is a very convenient technique for measuring the rate constants of slow chemical reactions involving the electrolysis products. As an

example, we shall consider the hydrolysis of *p*-benzoquinoneimine, formed by the anodic oxidation of *p*-aminophenol on a Pt electrode (Christensen and Anson [16]).

The anodic oxidation of *p*-aminophenol in aqueous solutions proceeds by the following mechanism [17–19]:

$$HO{-}C_6H_4{-}NH_2 - 2e \rightleftarrows O{=}C_6H_4{=}NH + 2H^+ ,$$
$$O{=}C_6H_4{=}NH + H_2O \rightarrow O{=}C_6H_4{=}O + NH_3 .$$

Fig. 6 shows a thin-layer chronopotentiogram of the oxidation of *p*-aminophenol followed by the reduction of *p*-benzoquinoneimine and *p*-benzoquinone.

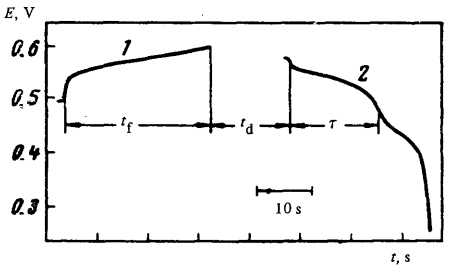


Figure 6. Thin-layer chronopotentiogram: *1*) oxidation of *p*-aminophenol, *2*) reduction of *p*-benzoquinoneimine and *p*-benzoquinone. t_d = 45.4 s.

p-Aminophenol (R) is oxidised during time t_f to *p*-benzoquinoneimine (O), which is then hydrolysed to *p*-benzoquinone (Z) by an irreversible first-order reaction. Since the reduction of *p*-benzoquinone occurs in a different region of potentials, this compound can be treated as electrochemically inert. The current is interrupted during the interval t_d, and the hydrolysis of *p*-benzoquinoneimine is the only possible reaction during this time. The polarity of the current is then reversed, and any unchanged *p*-benzoquinoneimine is reduced back to *p*-aminophenol (R). The hydrolysis reaction continues, in parallel with the reduction of *p*-benzoquinoneimine.

We shall calculate first of all the concentration of O in the thin layer of solution at time t ($0 < t < t_f$). We can write

$$\frac{dc_O}{dt} = \beta - kc_O \qquad (6)$$

where $\beta = i/nFAl$ (see Eqn. (1)). The first term in the right-hand side of Eqn. (6) describes the production of O, the second term describes its removal by the hydrolysis reaction.

Since $c_O = 0$ at $t = 0$, the solution of Eqn. (6) is

$$c_O = \frac{\beta}{k}(1 - e^{-kt}) . \qquad (7)$$

During the period when $i = 0$, i.e. for $t_f < t < t_f + t_d$, we can write

$$\frac{dc_O}{dt} = -kc_O . \qquad (8)$$

Solving Eqn. (8) and substituting for c_O from Eqn. (7), the following expression applies for $t' = t - t_f = 0$ (i.e. at the instant t_f):

$$c_O = \frac{\beta}{k} e^{-kt'}(1 - e^{kt_f}) . \qquad (9)$$

During the period of reduction of O, i.e. for $t_f + t_d < t < t_f + t_d + \tau$, we have

$$\frac{dc_O}{dt} = -\theta\beta - kc_O \qquad (10)$$

where θ is the ratio of cathodic to anodic current.

Solving Eqn. (10) and taking c_O from Eqn. (9) with $t'' = t - (t_f + t_d) = 0$ (i.e. at the instant t_d) we obtain

$$c_O = \frac{\beta}{k}\{e^{-kt''}[\theta + e^{-kt_d}(1 - e^{-kt_f})] - \theta\} . \qquad (11)$$

The transient time is determined by the condition $c_O = 0$, $t'' = \tau$. Hence, from Eqn. (11),

$$\tau = \frac{1}{k}\ln\left[1 + \frac{1}{\theta}e^{-kt_d}(1 - e^{-kt_f})\right] , \qquad (12)$$

and for $\theta = 1$

$$\tau = \frac{1}{k}\ln[1 + e^{-kt_d}(1 - e^{-kt_f})] . \qquad (13)$$

The theory for an analogous electrode process but in the usual chronopotentiometric model is much more complicated. The correctness of Eqn. (13) has been confirmed experimentally: Table 2 shows the results of measurements of the rate constant for the hydrolysis of *p*-benzoquinoneimine in 1.017 M H_2SO_4 at 25°C. The concentration of the starting material, *p*-aminophenol, was 1.01×10^{-2} M.

Table 2. Rate constant for the hydrolysis of *p*-benzoquinoneimine.

t_f, s	t_d, s	τ, s	10^3k, s^{-1}
32.1	9.9	23.9	7.8
41.8	19.9	28.1	7.3
19.0	42.2	12.7	7.0
27.4	45.4	16.6	7.5
36.0	50.4	20.3	7.3
16.6	51.1	10.3	7.4

Average $k = 7.4 \times 10^3$ s^{-1}

The equation for the rate constants of slow chemical reactions is greatly simplified by using the thin-layer cyclic potentiostatic method instead of the chronopotentiometric method. In that method, the unstable form is obtained under potentiostatic conditions, and the current (or the quantity of electricity) is plotted against time. After a certain time the potential is changed to a value at which the unstable product which has not yet reacted is converted back into the original form by the reverse electrochemical reaction. Oglesby and coworkers [20] used this method to study the acid-catalysed rearrangement of hydrazobenzene. The starting compound was the stable azo-form, and the unstable hydrazo-form was produced at the surface of the working electrode. The reaction mechanism is

$$C_6H_5{-}N{=}N{-}C_6H_5 + 2e + 2H^+ \rightleftarrows C_6H_5{-}NH{-}NH{-}C_6H_5 \xrightarrow{k} H_2N{-}C_6H_4{-}C_6H_4{-}NH_2 .$$

Theoretically, the time for complete exhaustion of a layer of solution 2×10^{-3} cm thick is less than one second[21]. If the reaction of interest is sufficiently slow, the unstable product may be formed rapidly in the potentiostatic experiment and allowed to react at the same potential during a much longer time (t_r) than the time required to generate it. The ratio of the quantities of electricity passed in the reverse and the forward electrolysis (h_r/h_b) is equivalent to the ratio of the initial concentration of reactant (e.g. azobenzene) to the final concentration of the product (e.g. hydrazobenzene). The plot of $\ln(h_r/h_b)$ against t_r for a first-order reaction should be a straight line of slope k.

When one-half of the product has reacted, $h_r/h_b = 2$. If we denote the time for half-reaction by $t_{1/2}$, the rate constant can be expressed in the form

$$k=\frac{\ln 2}{t_{1/2}}=\frac{0.693}{t_{1/2}}\ . \qquad (14)$$

The rate constants for the rearrangement of hydrazobenzene obtained by thin-layer methods agree satisfactorily with the values given by other electrochemical methods. Thus, the cyclic galvanostatic method gives 10.2×10^{-3} s^{-1}, the potential jump reversal method gives 10.7×10^{-3} s^{-1}, whereas the thin-layer chronopotentiometric and potentiostatic methods give 18.6×10^{-3} and 11.7×10^{-3} s^{-1} respectively. The concentration of $HClO_4$ was 0.075 M in every case.

(*d*) Study of adsorption

By virtue of its large ratio of electrode surface area to volume of solution, the thin-layer electrochemical cell can be used to study surface phenomena such as adsorption processes. Hubbard and Anson[3] have suggested a simple and convenient method for the quantitative determination of adsorbed materials from theoretical considerations of the behaviour of electrically active substances under the conditions of the thin-layer experiment.

If the compound is adsorbed on the electrode surface, and if the geometry of the cell justifies ignoring the second term in the right-hand side of Eqn. (2), the transient time which characterises the full exhaustion of the depolariser (whether adsorbed or not) can be expressed as

$$\tau=\frac{nFAlc}{i}+\frac{2nFA\Gamma}{i}\ , \qquad (15)$$

where Γ is the amount adsorbed in mole cm^{-2}. The coefficient 2 arises from the fact that adsorption occurs on both electrodes, each of area A. If the adsorbate does not take part in the electrode reaction under conditions leading to reaction by non-adsorbed species, the amount of adsorbate is found from the difference between the experimentally measured quantity of electricity and the quantity of electricity theoretically calculated by Eqn. (5).

The advantages of thin-layer electrochemistry in studies of adsorption phenomena have been demonstrated in a series of papers[22-24] on the adsorption of iodine. It is shown that the adsorption of I_2 and I^- on platinum electrodes can take two forms: an electrochemically active and an inactive state. Initially I_2 is adsorbed in the inactive form (up to $\sim 2\times10^{-9}$ mole cm^{-2}); this is followed by adsorption in the active form (a further 10^{-9} mole cm^{-2}).

Adsorbed, active I^- ($\sim 1.2\times10^{-9}$ mole cm^{-2}) blocks the adsorption of the inactive forms of I_2 and I^-. Adsorbed, inactive I_2 prevents further adsorption of I^-.

The adsorption of active I_2 is unaffected by whether the electrode is covered with I^- ions or by free iodine. The adsorption of inactive I^- can be estimated from the equations for the anodic transient time of the oxidation of I^- to I_2.

The presence of inactive, adsorbed I_2 can be confirmed by oxidative desorption ($n = 5$), followed by estimation of the resulting iodate.

In a study of the behaviour of the I_2/I^- couple it was found that the adsorbed iodide ion is not oxidised at potentials sufficient to oxidise non-adsorbed iodide.

These results suggest that adsorbed I^- and I_2 are not likely to be the species responsible for the electron transfer reactions giving rise to the exchange current at Pt electrodes in I^-/I_2 solutions. Workers who reached the opposite conclusion[25,26] from their kinetic studies must have argued incorrectly.

The conclusions made from the study of the electrochemical behaviour of the I_2/I^- couple on Pt electrodes in thin layers of solution are somewhat inconsistent with conclusions based on other methods[27-33]. However, some aspects of the thin-layer work[22-24] are not entirely convincing, and should be re-examined.

2. Voltammetry

(*a*) Reversible processes

If a depolariser is present in the thin layer of solution, the application of a prescribed potential to the electrode will cause a current to flow through the cell as a result of the electrochemical reaction. The layer of solution immediately adjacent to the electrode surface will be gradually depleted of depolariser; however, a new supply of depolariser is available by diffusion from within the solution. This process produces a thickening of the diffusion layer, which in the thin-layer experiment cannot exceed the value l. On raising the electrode potential the rate of the electrochemical process increases, but at the same time the supply of depolariser is hindered. As a result, the current increases only to a certain value, and then decreases to zero. Anson and Hubbard[34] have derived an equation which describes the current–voltage characteristic of the process, assuming that the electrode potential is varied linearly with time.

For a reversible reaction ($O + ne \rightleftharpoons R$) and a relatively slow rate of change of potential (not more than 20 mV s^{-1}), the following expressions for c_O and c_R can be used:

$$c_O=c_O^0\left\{1/\left[1+\exp\frac{nF}{RT}(E^0-E)\right]\right\}\ , \qquad (16)$$

$$c_R=c_R^0\left\{1/\left[1+\exp\frac{nF}{RT}(E-E^0)\right]\right\}\ . \qquad (17)$$

The current i flowing through the thin-layer cell when the potential is scanned cathodically can be calculated from the expression

$$i=-nFV\frac{dc_O}{dt}\ . \qquad (18)$$

The expression for the cathodic voltammetric curve can be obtained from Eqns. (16) and (18):

$$i=n^2Vrc_O^0\frac{F^2}{RT}\left\{\frac{\exp\frac{nF}{RT}(E^0-E)}{\left[\exp\frac{nF}{RT}(E^0-E)+1\right]^2}\right\}. \qquad (19)$$

The thin-layer voltammetric curve is bell-shaped and symmetrical about the peak potential (see Fig. 7). The current maximum (i_p) is associated with the potential E^0, and is given by the expression

$$i_p = \frac{n^2 c_O^0 r V F^2}{4RT} . \quad (20)$$

The simplicity of the theory of thin-layer voltammetry in comparison with oscillographic polarography is clearly brought out by comparing Eqn. (19) with the Randles–Ševčik equation[35,36].

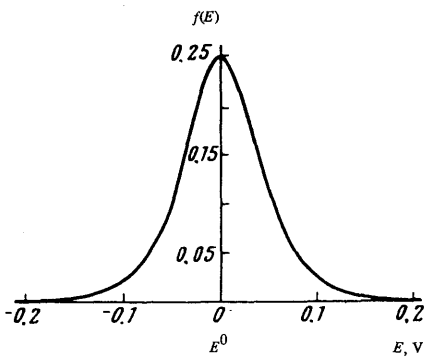


Figure 7. Theoretical i–E voltammetric curve for a reversible process in a thin-layer cell:

$$f(E) = \frac{\exp\left[\frac{F}{RT}(E - E^0)\right]}{\left\{\exp\left[\frac{F}{RT}(E - E^0)\right] + 1\right\}^2} .$$

Comparing the equation for the peak current in normal oscillographic voltammetry,

$$i_p = \frac{0.452 n^{3/2} F^{3/2} c_O^0 D^{1/2} r^{1/2} A}{R^{1/2} T^{3/2}} \quad (21)$$

with Eqn. (20), it can be seen that the current density in thin-layer voltammetry is significantly lower:

$$\frac{i_p}{(i_p)_{tl}} = \left(\frac{RT}{nF}\right)^{1/2} \frac{1.808 D^{1/2}}{r^{1/2} l} = \frac{0.286 D^{1/2}}{n^{1/2} r^{1/2} l} \quad (22)$$

whence $i_p/(i_p)_{tl} = 22$ if $n = 1$, $r = 10^{-3}$ V s^{-1}, $l = 10^{-3}$ cm, and $D = 6 \times 10^{-6}$ cm^2 s^{-1}. However, with small values of r and stationary electrodes these smaller currents can be measured as accurately as the currents encountered in oscillographic polarography, where the large value of r gives rise to substantial capacitive currents.

(*b*) Irreversible processes

Thin-layer voltammetry is very convenient for the study of irreversible reactions[37] ($O + ne \rightarrow R$).

The voltammetric curve for an irreversible system is asymmetric about the peak potential E_p, and the peak potential and its height (peak current) are related to the kinetic parameters k^0 and αn_0 by simple expressions.

We start from the basic equation of electrochemical kinetics, which describes both the forward and the reverse reaction

$$i = nFAk^0 \left\{c_O \exp\left[\frac{-\alpha n_0 F}{RT}(E - E^0)\right] - c_R \exp\left[\frac{(1-\alpha) n_0 F}{RT}(E - E^0)\right]\right\} . \quad (23)$$

If the peak current is at least two orders of magnitude greater than the exchange current the contribution of the reverse reaction to the voltammetric curve is negligible, and we can write

$$i = nFAk^0 c_O \exp\left[(-\alpha n_0 F/RT)(E - E^0)\right] . \quad (24)$$

Combining Eqns. (18) and (24) we obtain

$$\frac{dc_O}{dt} = -\frac{Ak^0 c_O}{V} \exp\left[\frac{-\alpha n_0 F}{RT}(E - E^0)\right] . \quad (25)$$

Integration of Eqn. (25) affords an expression for c_O. Inserting it into Eqn. (24), we arrive at an expression for the cathodic i, E curve in terms of the initial concentration only:

$$i = nFAk^0 c_O^0 \exp\left\{\frac{-\alpha n_0 F}{RT}(E - E^0) - \frac{ARTk^0}{\alpha n_0 FV(-r)} \exp\left[\frac{-\alpha n_0 F}{RT}(E - E^0)\right]\right\} . \quad (26)$$

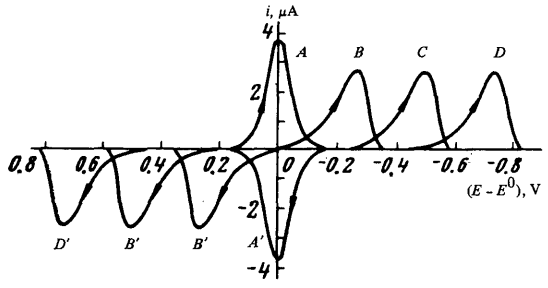


Figure 8. Theoretical voltammetric curves for a reversible reaction and for fully irreversible reactions in a thin layer of solution: *A*) reversible reaction, $k^0 \geq 4 \times 10^{-3}$ cm s^{-1}, *B*)–*D*) fully irreversible reactions, $k^0(B) = 10^{-6}$, $k^0(C) = 10^{-8}$, $k^0(D) = 10^{-10}$ cm s^{-1}. ($\alpha n_0 = 0.5$, $V = 2 \times 10^{-3}$ cm^3, $|r| = 2 \times 10^{-3}$ V s^{-1}, $n = 1$, $A = 0.5$ cm^2, $C^0 = 10^{-6}$ mole cm^{-3}, $T = 298$°K).

Fig. 8 shows plots of Eqn. (26) for several values of k^0 and one value of αn_0. It can be seen that the shape of the curves is independent of k^0, the curves being merely shifted along the potential axis. However, the peaks become broader and flatter if αn_0 decreases (Fig. 9).

The equations for the cathodic peak potential and for the peak current are obtained by equating to zero the differential di/dE from Eqn. (26).

The peak potential depends on αn_0 and on k^0, but is independent of concentration

$${}_cE_p = E^0 - (2.3RT/\alpha n_0 F) \lg\left[\alpha n_0 F(-r)V/ARTk^0\right] \quad (27)$$

whereas the peak current is directly proportional to αn_0 and to concentration

$${}_ci_p = \alpha n_0 n F^2 V(-r) c_O^0/2.718RT . \quad (28)$$

From Eqn. (28) we can calculate αn_0, and hence we can find k^0 from Eqn. (27) if E^0 is known.

Eqns. (27) and (28) can be applied to an anodic reaction by replacing α by $(1-\alpha)$ and c_O^0 by c_R^0.

If a cyclic voltammetric curve is plotted, the same kinetic parameters can be obtained without a knowledge of E^0. In this case we write equations for ${}_cE_p$ and ${}_aE_p$, from which E^0 can be eliminated. The final expression for k^0 is

$$k^0 = \left\{\frac{2.718\,{}_ci_p}{nFAc^0}\left(\frac{-2.718\,{}_ai_p}{nFAc^0}\right)^{{}_ci_p/{}_ai_p}\cdot\exp\left[\frac{-2.718\,{}_ci_p}{nFV|r|c^0}({}_aE_p-{}_cE_p)\right]\right\}^{{}_ai_p/({}_ai_p-{}_ci_p)}. \quad (29)$$

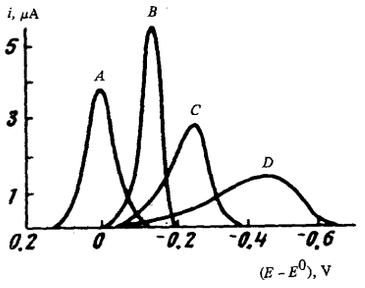


Figure 9. Theoretical voltammetric curves for a reversible reaction and for fully irreversible reactions in a thin layer of solution for different values of αn_0: *A*) reversible reaction, *B*)–*D*) irreversible reactions; $\alpha n_0(B) = 0.75$, $\alpha n_0(C) = 0.50$, $\alpha n_0(D) = 0.25$. ($k^0 = 10^{-6}$ cm s^{-1}, all other parameters as in Fig. 8).

For $\alpha n_0 = 0.5$ and ${}_ci_p = {}_ai_p$, Eqn. (29) simplifies to

$$\lg k^0 \overset{a}{=} -(1260/T)({}_aE_p - {}_cE_p) + \lg(VF|r|/2ART). \quad (30)$$

An equation for α can be obtained by eliminating n_0 from equations for ${}_ci_p$ and ${}_ai_p$ of the type of Eqn. (28). For $c_O^0 = c_R^0$ we have

$$\alpha = {}_ci_p/({}_ci_p - {}_ai_p). \quad (31)$$

Thus, α and n_0 can be evaluated separately in cyclic thin-layer voltammetry, but of course only if n_0 is the same for the cathodic and the anodic process.

Eqn. (26) describes the current–voltage curve of an irreversible reaction with a relative error of 2% if the exchange current does not exceed 2% of the peak current.

Thus, using the equation

$$i_0 = nFAk^0c \quad (32)$$

to calculate the maximum value of the exchange current i_0, and Eqn. (28) to calculate the smallest value of the peak current i_p, we obtain

$$i_0/i_p = 2.718ARTk^0/\alpha n_0FVr > 0.02 \quad (33)$$

or

$$k^0 < (\alpha n_0FV|r|/2.718ART)\cdot 0.02\ . \quad (34)$$

For normal values of the experimental parameters ($\alpha n_0 = 0.5$; $V = 2\times10^{-3}$ cm^3; $|r| = 2$ mV s^{-1}; $T = 298$°K; $A = 0.5$ cm^2) we obtain $k^0 < 1.2\times10^{-6}$ cm s^{-1}.

Hence, Eqn. (26) is applicable to fully irreversible processes, having rate constants of the order of 10^{-6} or less.

Eqn. (19) describes the current–voltage curve for a reversible reaction, with a relative error of 2%, for the condition

$$i_0/i_p = 4ARTk^0/nFV|r| > 50\ . \quad (35)$$

This condition is satisfied if

$$k^0 > (nFVr/4RTA)\cdot 50 \quad (36)$$

With the values of the parameters assumed above, we obtain $k^0 < 4\times10^{-3}$ cm s^{-1}. Hence, a "reversible" reaction is a reaction whose rate constant does not exceed 4×10^{-3} s^{-1}.

(*c*) Effect of double layer structure

All the above equations have been obtained without allowing for the effect of the structure of the electrical double layer. The basic equation of electrochemical kinetics which allows for the effect of the double layer on the surface concentration of the depolariser is

$$i = nFAk^0c_O^0f(\psi_1)\exp[(-\alpha n_0F/RT)(E-E^0)] \quad (37)$$

where $f(\psi_1) = \exp[(\alpha n_0 - z_0)(F/RT)\psi_1]$, and z_0 is the charge on a particle of the substance under study.

The equation for the cathodic i–E curve follows from Eqns. (26) and (37):

$$i = nFAk^0c_O^0f(\psi_1)\exp\left\{\frac{-\alpha n_0F}{RT}(E-E^0) + \frac{Ak^0}{V(-r)}\int_{E_i}^{E} f(\psi_1)\exp\left[-\frac{\alpha n_0F}{RT}(E-E^0)\right]dE\right\} \quad (38)$$

where E_i is the potential at which the scan is started.

Assuming that the electrode potential is divided between two capacitances in series, the fixed (C) and the diffuse (C_d) parts of the double layer, and assuming these capacitances to be independent of potential over the narrow range of potential for which the current is fairly large (about $200/n$ mV), we can write

$$\psi_1 \simeq (C/C_d)(E-\varphi_0) \quad (39)$$

where φ_0 is the zero-charge potential.

Combining Eqns. (38) and (39),

$$i = nFAk^0c_O^0f(\psi_1)\exp\left\{\frac{-\alpha n_0F}{RT}(E-E^0) - \frac{ARTk^0}{FV(-r)}\,\frac{f(\psi_1)\exp\left[\frac{-\alpha n_0F}{RT}(E-E^0)\right]}{[\alpha n_0 + (z_0-\alpha n_0)C/C_d]}\right\}. \quad (40)$$

The equation for the peak potential is

$${}_cE_p = \frac{\alpha n_0E^0 + (z_0-\alpha n_0)\frac{C}{C_d}\varphi_0 - \frac{RT}{F}\ln\left\{\frac{FV(-r)}{ARTk^0}\left[\alpha n_0 + (z_0-\alpha n_0)\frac{C}{C_d}\right]\right\}}{\alpha n_0 + (z_0-\alpha n_0)C/C_d}. \quad (41)$$

Eqn. (41) reduces to Eqn. (27) when C is much smaller than C_d. (This case is found in the presence of an excess of indifferent electrolyte.) Eqns. (38) and (40) are fully analogous to Eqn. (26) except for the function $f(\psi_1)$ which replaces the factor $\exp[(-\alpha n_0F/RT)\cdot(E-E^0)]$ in Eqn. (40). Taking Eqn. (39) into account, the product $f(\psi_1)\exp[(-\alpha n_0F/RT)\cdot(E-E^0)]$ becomes

$$f(\psi_1)\exp\left[\frac{-\alpha n_0F}{RT}(E-E^0)\right] = \exp\left\{\frac{F}{RT}\left[\frac{C}{C_d}(z_0-\alpha n_0)\cdot\varphi_0 + \alpha n_0E^0\right]\right\}\exp\left[\alpha^*\frac{F}{RT}E\right] \quad (42)$$

where

$$\alpha^* = (z_0-\alpha n_0)C/C_d + \alpha n_0\ . \quad (43)$$

Finally, the peak current with allowance for the effect of double layer structure is given by

$${}_ci_p = \alpha^*nF^2V(-r)c_O^0/2.718RT\ . \quad (44)$$

It follows from Eqns. (43) and (44) that α^* (and therefore also c^i_p) should be smaller for anion reactions than for cation reactions. Thin-layer i–E curves for intermediate and low concentrations of indifferent electrolyte contain information on the ratio C/C_d.

(*d*) Multistage processes

If a compound is reduced in two fully irreversible steps, for example

$$(PtCl_6)^{2-} + 2e \xrightarrow{k_1^0} (PtCl_4)^{2-} + 2Cl^-$$

and

$$(PtCl_4)^{2-} + 2e \xrightarrow{k_2^0} Pt + 4Cl^- \ ,$$

the current–voltage curve (Fig. 10) should have two peaks if the first step is the faster (curve *A*), or one peak if the second step is the faster or if the two steps have comparable rates (curves *B* and *C*).

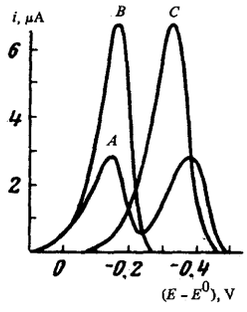


Figure 10. Theoretical thin-layer curves for a two-step fully irreversible reaction: *A*) $k_1^0 = 10^{-5}$, $k_2^0 = 10^{-7}$; *B*) $k_1^0 = k_2^0 = 10^{-5}$; *C*) $k_1^0 = 3 \times 10^{-7}$, $k_2^0 = 10^{-5}$ cm s^{-1} (all other parameters as in Fig. 8).

If $k_1^0 \geq 10^3 k_2^0$ the equations presented in the previous sub-sections can be used to describe both steps.

The basic i–E equation for a fully irreversible, two-step reaction such as

$$O + n_1 e \rightarrow R_1$$
$$R_1 + n_2 e \rightarrow R_2$$

but without allowance for the influence of the double-layer structure is obtained as follows. The contribution to the current from the first step is expressed by Eqn. (26):

$$i_1 = n_1 F A k_1^0 c_1^0 \exp\left\{\frac{-(\alpha n_0)_1 F}{RT}(E - E_1^0)\frac{-ART k_1^0}{(\alpha n_0)_1 FV(-r)} \cdot \exp\left[\frac{-(\alpha n_0)_1 F}{RT}(E - E_1^0)\right]\right\}. \quad (45)$$

The current associated with the second step is given by

$$i_2 = -n_2 FV\frac{dc_2}{dt} + i_1 = n_2 F A c_2^0 k_2^0 \exp\left[\frac{-(\alpha n_0)_2 F}{RT}(E - E_0^0)\right]. \quad (46)$$

Eqn. (46) is solved for c_2 and i_2 using the normal methods for linear first-order differential equations

$$c_2 = c_1^0 H^{-1}\int_{E_i}^{E} GH dE \ , \quad (47)$$

$$i_2 = n_2 F A k_2^0 c_1^0 H^{-1} \exp\left[\frac{-(\alpha n_0)_2 F}{RT}(E - E_2^0)\int_{E_i}^{E} GH dE\right] , \quad (48)$$

where

$$G = \frac{n_1 A k_1^0 c_1^0}{n_2 Vr}\exp\left\{\frac{-(\alpha n_0)_1 F}{RT}(E - E_1^0) + \frac{Ak_1^0 RT}{(\alpha n_0)_1 FVr}\exp\left[\frac{-(\alpha n_0)_1 F}{RT}(E - E_1^0)\right]\right\},$$

$$H = \exp\{[Ak_2^0 RT/V(-r)(\alpha n_0)_2 F]\exp[(-(\alpha n_0)_2 F/RT)(E - E_2^0)]\} ,$$

c_1^0 is the initial concentration of O and c_2^0 is the initial concentration of R_1. Since the total current is $i = i_1 + i_2$, the expression for the i–E curve becomes

$$i = n_2 FVrc_1^0 G + n_2 F A k_2^0 c_1^0 H^{-1}\exp\left[\frac{-(\alpha n_0)_2 F}{RT}(E - E_2^0)\int_{E_i}^{E} GH dE\right] . \quad (49)$$

The integral term in the right-hand side of Eqn. (49) cannot be solved analytically. Plots obtained by numerical integration for $(\alpha n_0)_1 = (\alpha n_0)_2 = 0.5$ and several pairs of values of k_1^0 and k_2^0 are reproduced in Fig. 10.

(*e*) Partially reversible reactions

The current–voltage curve for fast but not fully reversible reactions, in which the contribution of the reverse reaction cannot be neglected, is described by the equation

$$i = -nFA\left\{k_b c_O^0 - \frac{Ac_O^0}{Vr}(k_f + k_b)X^{-1}\int_{E_i}^{E} X k_b dE\right\} \quad (50)$$

where

$$X = \exp\{[ART/V(-r)n_0 F][k_f/\alpha - k_b/(1-\alpha)]\} ,$$

$$k_f = k^0 \exp[(-\alpha n_0 F/RT)(E - E^0)] ,$$

$$k_b = k^0 \exp\{[(1-\alpha)n_0 F/RT](E - E^0)\} .$$

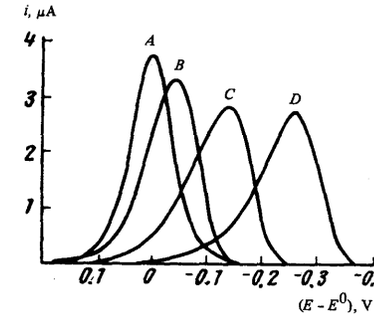


Figure 11. Theoretical voltammetric curves for reactions of intermediate reversibility in a thin layer: $k^0(A) = 4 \times 10^{-3}$, $k^0(B) = 10^{-4}$, $k^0(C) = 10^{-5}$, $k^0(D) = 10^{-6}$ cm s^{-1} (all other parameters as in Fig. 8).

An analogous equation for anodic reactions is obtained from Eqn. (50) by replacing c_O^0 by c_R^0. A plot of Eqn. (50) is shown in Fig. 11. The size of the current peak is intermediate between those given by Eqns. (20) and (28) for reversible ($k^0 > 4 \times 10^{-3}$ cm s^{-1}) and fully irreversible ($k^0 > 1 \times 10^{-6}$ cm s^{-1}) reactions respectively.

(*f*) Competitive reactions

When the starting material can undergo two parallel, fully irreversible reactions, as in

$$O + n_1 e \rightarrow R_1 ,$$
$$O + n_2 e \rightarrow R_2 ,$$

the shape of the current–voltage curve (Fig. 12) differs from that of the corresponding curve for a reaction which takes place by a single path (Fig. 8). In spite of the presence of two reactions, a single peak is obtained. The current–voltage characteristic for an electrode process of this type is derived as follows. The current in this case is given by

$$i = FAc_O (n_1 {}_1k_f + n_2 {}_2k_f) \quad (51)$$

where

$${}_1k_f = {}_1k^0 \exp\{[-(\alpha n_0)_1 F/RT](E - E_1^0)\},$$
$${}_2k_f = {}_2k^0 \exp\{[-(\alpha n_0)_2 F/RT](E - E_2^0)\} .$$

The current must also obey the equation

$$i = -FV\left(\frac{n_{11}k_f + n_2 {}_2k_f}{{}_1k_f + {}_2k_f}\right)\frac{dc_O}{dt} \quad (52)$$

The quantity in brackets in the right-hand side of Eqn. (52) is the instantaneous effective value of n for the mixed reaction. Eqns. (51) and (52) are easily solved:

$$i = FAc_O^0(n_1 {}_1k_f + n_2 {}_2k_f)\exp\left\{\frac{ART}{VFr}\left[\frac{{}_1k_f}{(\alpha n_0)_1} + \frac{{}_2k_f}{(\alpha n_0)_2}\right]\right\} . \quad (53)$$

Plots of Eqn. (53) are given in Fig. 12.

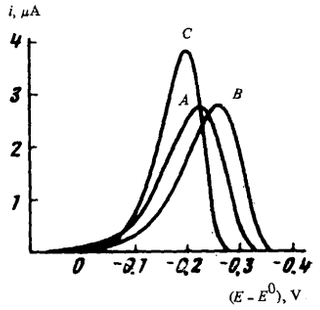


Figure 12. Theoretical voltammetric curves for two parallel reactions: *A*) $E_1^0 = E_2^0 = 0.0$, $(\alpha n_0)_1 = (\alpha n_0)_2 = 0.5$; *B*) $E_1^0 = 0.0$, $E_2^0 = -0.20$, $(\alpha n_0)_1 = (\alpha n_0)_1 = 0.5$; *C*) $E_1^0 = 0.0$, $E_2^0 = 0.20$, $(\alpha n_0)_1 = 0.7$, $(\alpha n_0)_2 = 0.5$. ($n_1 = n_2 = 1$, $k^0 = 10^{-6}$ cm s^{-1}, $c_O^0 = 10^{-6}$ mole cm^{-3}, all other parameters as in Fig. 8).

(*g*) Practical applications

The cyclic thin-layer voltammetric method has been used to study the adsorption on platinum of complex ions in the Co^{3+}/Co^{2+}–EDTA‡ and Fe^{3+}/Fe^{2+}–EDTA systems[22]. The Co^{3+}/Co^{2+}–EDTA couple is appreciably irreversible; addition of iodide ions makes the reaction almost reversible (Fig. 13). A probable explanation is that the preferred adsorption of iodide ions causes desorption of the cobalt complexes which inhibit the electrode reaction when they are adsorbed. This property of the iodide ion has been used[22] for the quantitative determination of cobalt complexes, which are readily adsorbed on a smooth platinum surface[38,39]. The full desorption of the cobalt complexes from the platinum surface by the I^- was demonstrated by the following experiment: 0.94 μl of the sample (10^{-3} M CoY^- or CoY^{2-} in 1 M phosphate buffer, pH 7) was introduced into the clean thin-layer cell. The volume of the interelectrode gap was exactly equal to the volume of solution. The distance between the electrodes was first increased to 2–3 mm, and 0.94 μl of 2×10^{-3} M solution of KI was added to the initial solution. The volume of the gap was then decreased to 1.88 μl, and the cobalt complexes were determined. The results are given in Table 3.

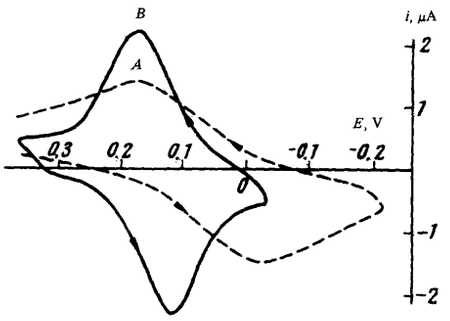


Figure 13. Single-cycle thin-layer voltammetric curve for Co^{3+} and Co^{2+} complexes with EDTA: *A*) without added iodide, 1.77×10^{-3} ml of 1.0 mM Co^{3+}–EDTA in 1 M (pH 7) phosphate buffer; *B*) with added iodide, 1.4×10^{-3} ml of 1.0 mM Co^{3+}–EDTA in 1 M $NaClO_4$ (pH 5) + 1.0×10^{-3} ml 2.0 nM solution of KI. Sweep rate 2 mV s^{-1}.

Table 3. Desorption of CoY^- and CoY^{2-} from a platinum surface by iodide ions.

No. of experiments	total quantity of electricity measured experimentally, Q_{tot} microcoulombs	quantity of electricity in blank experiment, Q_x microcoulombs	$Q_{tot} - Q_x$ microcoulombs	theoretical value of Q microcoulombs
Reduction of CoY^- (Co^{3+}-EDTA)				
6	106±3	14±2	92±5	91
Oxidation of CoY^{2-} (Co^{2+}-EDTA)				
5	115±6	24±2	91±8	91

The scanning range of potential was from 0.25 to −0.05 V (relative to the normal calomel electrode) in the first case, from 0.00 to 0.3 V in the second case. The Q_x values were obtained by repeating the experiment with a solution of phosphate buffer to which no depolariser had been added. The fact that the cobalt complex is completely reduced indicates that the iodide ion itself has no electrochemical activity in this range of potentials.

‡EDTA is ethylenediaminetetra-acetate.

Conversely, the Fe^{3+}/Fe^{2+}–EDTA system is reversible even in the absence of iodide ions. Thus, the displacement of adsorbed ions by more surface-active particles can be used for the quantitative study of the adsorption of ions under thin-layer conditions.

Thin-layer voltammetry has been applied to the study of the stoichiometry of the electrochemical oxidation of $PtCl_4^{2-}$ and $PtBr_4^{2-}$, of the reduction of $PtCl_6^{2-}$ and $PtBr_6^{2-}$, and also of their hydrolysis products[40]. It has been shown that in acid solution the reduction of $PtCl_6^{2-}$ proceeds to the stage of $PtCl_4^{2-}$, and in neutral solutions or solutions free from chloride ions the reduction goes to metallic platinum. The reduction of $PtBr_6^{2-}$ in 1 M bromide solutions goes to $PtBr_4^{2-}$, and in acid solutions or solutions free from bromide ions the reduction goes to Pt. The oxidation of $PtCl_4^{2-}$ in 1 M chloride solutions apparently gives a mixture of $PtCl_6^{2-}$ and $Pt(OH)_2Cl_4^{2-}$, whereas the oxidation of $PtBr_4^{2-}$ in 1 M bromide solutions gives only $PtBr_6^{2-}$. It was also found that the hydrolysis products of $PtCl_6^{2-}$ and $PtBr_6^{2-}$ are reduced with greater ease than their parent complexes.

Thin-layer studies with a very slow voltage scan[34] give valuable information on the mechanism of electrode reactions.

Because of the lower current densities employed, the reversibility of the Cr^{3+}–Cr^{2+} couple under the conditions of thin-layer voltammetry is much better ($E_c = -0.8$, $E_a = -0.6$ V NCE) than under semi-infinite diffusion conditions ($E_c = -0.95$, $E_a = -0.45$ V NCE).[8]

The application of thin-layer voltammetry to the electrolytic oxidation of bivalent platinum complexes of the $Pt(NH_3)_m(NO_2)_{4-m}^{m-2}$ and $Pt(NH_3)_mCl_{4-m}^{m-2}$ type has shown[41,42] that the process is strongly catalysed by free chloride and iodide ions, and that some of the ligands in the reaction product (i.e. the Pt^{IV} complex) are replaced by chloride ions. In the absence of free chloride ions the reactivity of these complexes is strongly reduced.

3. Stead-state Current Method

The existence of a limiting diffusion current depends on the establishment of a steady-state concentration polarisation.

A limiting diffusion current is observed when the thickness of the diffusion layer does not change with time. These conditions are realised at a dropping mercury electrode or at a solid electrode moving relative to the solution. Paired, thin-layer electrolytic cells also enable a constant concentration gradient to be set up; the value of the gradient can be controlled by varying the interelectrode spacing.

Material obtained by reduction at one electrode of a paired cell can diffuse and be oxidised at the other working electrode. Since these processes take place in a closed system, a steady-state current can be obtained.

The formation of the steady-state current i_{ss} is illustrated in Fig. 14.[43] Initially, the potential applied to the working electrodes is made sufficiently negative to ensure that the solution is depleted of the oxidised form O. If the potential of one of the electrodes (the anode) is shifted towards positive values, oxidation of R will begin at some value of the anode potential; the concentration of the oxidised form will increase, and the concentration of the reduced form will decrease. The flow of each form across the thin layer towards the appropriate electrode can be expressed in terms of its surface concentration:

$$\frac{i_{ss}}{nFA} = D_R \frac{(c_R)_{x=0} - (c_R)_{x=l}}{l} = D_O \frac{(c_O)_{x=l}}{l} . \qquad (54)$$

The total number of moles of O and R contained in the thin layer between the electrodes is constant: $N_O + N_R = N$. Hence

$$\frac{lA\,(c_O)_{x=l}}{2} + \frac{lA\,[(c_R)_{x=0} + (c_R)_{x=l}]}{2} = N . \qquad (55)$$

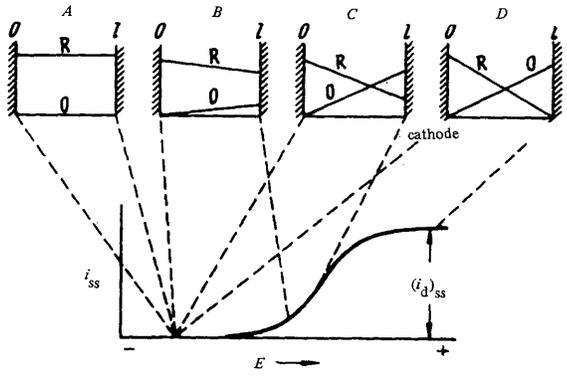


Figure 14. Schematic illustration of the formation of a steady-state current by reference to the concentration profiles of O and R in a thin layer for gradually increasing values of E at one of the electrodes (anode).

Solving Eqns. (54) and (55) simultaneously we obtain

$$(c_O)_{x=l} = \frac{i_{ss} l}{nFAD_O} , \qquad (56)$$

$$(c_R)_{x=l} = -\frac{i_{ss} l}{2nFA}\left(\frac{1}{D_R} + \frac{1}{D_O}\right) + \frac{N}{lA} , \qquad (57)$$

$$(c_R)_{x=0} = \frac{i_{ss} l}{2nFA}\left(\frac{1}{D_R} - \frac{1}{D_O}\right) + \frac{N}{lA} . \qquad (58)$$

When the anode potential becomes sufficiently positive $(c_R)_{x=l}$ vanishes and the current tends to a maximum value $(i_d)_{ss}$. Hence it follows from Eqn. (56) that

$$(i_d)_{ss} = \frac{nFADc}{l}$$
$$\text{where } c = c_O + c_R, \text{ and } D = \frac{2D_O D_R}{D_O + D_R} . \qquad (59)$$

Thus, the limiting steady-state current is directly proportional to a function of the diffusion coefficients of the oxidised and the reduced form, the total concentration, and the electrode area, and inversely proportional to the distance between the electrodes.

(*a*) Determination of the kinetic parameters of an electron transfer reaction

Steady-state currents can be used to determine the electron transfer rate constant k_S and the transfer coefficient α. In its most general form, the variation of the current with anode potential is given by

$$i_{ss} = nFAk_s\left\{(c_R)_{x=l} \exp\frac{(1-\alpha)\,nF\,(E-E^0)}{RT} + (c_O)_{x=l} \exp\left[\frac{-\alpha nF\,(E-E^0)}{RT}\right]\right\} . \qquad (60)$$

Replacing $\exp[-nF/RT(E-E^0)]$ by θ, and $(cO)_{x=l}$ and $(cR)_{x=l}$ by their values given by Eqns. (56) and (57), we obtain after some simplification

$$\frac{1}{\theta^{\alpha-1}lk_s}+\frac{\theta}{D_O}=\left[\frac{(i_d)_{ss}-i_{ss}}{i_{ss}}\right]\left(\frac{D_O+D_R}{2D_OD_R}\right) \quad (61)$$

This equation describes the variation of the steady-state current with anode potential when the concentration of the oxidised form at the cathode is zero, i.e. $(cO)_{x=0}=0$. Analogous expressions can be obtained for the cathode. If the second term in the left-hand side of Eqn. (61) is much greater than the first (i.e. if k_S is large) this equation reduces to the equation which describes the reversible behaviour of the material:

$$E_{anode}=E^0-\frac{RT}{nF}\ln\left(\frac{1}{2}+\frac{D_O}{2D_R}\right)-\frac{RT}{nF}\ln\left[\frac{(i_d)_{ss}-i_{ss}}{i_{ss}}\right]. \quad (62)$$

If, on the other hand, the first term in the left-hand side of Eqn. (61) is predominant (k_S small), the resulting equation describes the fully irreversible behaviour of the substance under study:

$$E_{anode}=E^0-\frac{RT}{(1-\alpha)nF}\ln\left[\frac{lk_s(D_O+D_R)}{2D_OD_R}\right]-\frac{RT}{(1-\alpha)nF}\ln\left[\frac{(i_d)_{ss}-i_{ss}}{i_{ss}}\right]. \quad (63)$$

The electron transfer rate constant k_S can be evaluated by plotting $\lg\left[\frac{(i_d)_{ss}-i_{ss}}{i_{ss}}\right]$ against E. The plot is a straight line of slope $2.3RT/(1-\alpha)nF$, intersecting the horizontal axis at the potential

$$E^0-[2.3RT/(1-\alpha)nF]\lg\{[lk_s(D_O+D_R)]/2D_OD_R\}.$$

As in other methods, k_S can be found if E^0 is known. To find the rate constant k_S we may use the following approach. If the quantity $\left[\frac{(i_d)_{ss}-i_{ss}}{i_{ss}}\right]$ is plotted against $1/l$ for a series of anodic potentials, we should obtain (according to Eqn. (61)) a family of straight lines of slope $2D_OD_R/[\theta^{\alpha-1}k_S(D_O+D_R)]$, intersecting the vertical axis at the ordinate $2D_R\theta/(D_O+D_R)$. When the intercept is equal to $2D_R/(D_O+D_R)$, and therefore $\theta=1$, the value of k_S can be found from the slope at $E=E^0$. The value of α can then be found from the other curves.

(b) Determination of the diffusion coefficient

Since the steady-state current, according to Eqn. (54), depends on the diffusion coefficients of the oxidised and the reduced form, the equation can be used to evaluate these coefficients. If the concentrations of the oxidised form at $x=0$ and of the reduced form at $x=l$ are zero, Eqn. (54) can be re-written

$$(i_d)_{ss}=nFAD_R\frac{(c_R)_{x=0}}{l}=nFAD_O\frac{(c_O)_{x=l}}{l}. \quad (64)$$

Eqn. (64) can be used to determine the diffusion coefficients from a knowledge of the limiting steady-state current, the concentrations at the electrodes, the electrode area, and the distance between the electrodes. The number of moles of O and R in the thin layer can be measured coulometrically. If one of the electrodes of the thin-layer cell is disconnected (for example, the anode) the current will flow only to the cathode and as long as oxidised material remains in the thin layer. By measuring the quantity of electricity used in the reduction of O, and inserting $Q_c=nFAlc_O$ in Eqn. (64), we obtain

$$D_O=(i_d)_{ss}l^2/2Q_c \quad (65)$$

D_R can be expressed in a similar way.

The numerical values of the diffusion coefficients are obtained from the slopes of plots of l against $1/i_{ss}$ and l against Q. The diffusion coefficients for Fe^{2+} and Fe^{3+} in 0.1 M $HClO_4$, measured by this method, are 0.421×10^{-5} and 0.392×10^{-5} cm^2 s^{-1} respectively; those for benzoquinone and hydroquinone in 0.3 M $HClO_4$ are 1.15×10^{-5} and 1.16×10^{-5} cm^2 s^{-1}.

(c) Determination of the rate constants of chemical reactions

The rate constants of chemical reactions can be determined from measurements of steady-state currents.

For slow chemical reactions of the type

$$O+ne\rightleftarrows R;\ mR+pZ\xrightarrow{k}F$$

we can use the expression

$$i_{ss}=nFAlk(R_{ss})^m(Z)^p \quad (66)$$

where R_{SS} is the steady-state concentration of the reduced form. Under normal conditions ($n=2$, $lA=2\times10^{-3}$, $k(Z)^p=10^{-1}$, $R_{SS}=10^{-6}$) the system will reach steady state in 10 s for a current of 4×10^{-5} A. R_{SS} can be evaluated by anodic scanning and integration of the current associated with the fast oxidation of the substance R. Introducing into Eqn. (66) the quantity of electricity Q_R consumed by the oxidation of R_{SS}, we can write

$$i_{ss}=nFAk\left(\frac{Q_R}{nFA}\right)^m(Z)^p\left(\frac{1}{l^{m-1}}\right). \quad (67)$$

If the reaction is of the first order with respect to R, it follows from Eqn. (67) that the slope of the plot of Q_R against i_{SS} is independent of l. In this case we can determine p from experiments at different concentrations of the component Z, and hence we can arrive at the rate constant.

If the kinetic order of the reaction is 2 or more, the slope of plots of $(Q_R)^m$ against i_{SS} is a function of l, but the dependence is always one order less than in plots of $(R_{SS})^m$ against i_{SS}, as in Eqn. (66). The upper limit of the rate of a pseudo-first order reaction, measured by this method, depends on the rate of diffusion. Assuming that the concentration of R must be constant to within 1% the highest value of k which can be measured by this method is 10^{-1} s^{-1}.

To measure very small reaction rates, we need a high concentration (R_{SS}) and a large interelectrode distance, so as to raise i_{SS} above the level of the background current. For the highest reasonable values ($R_{SS}=10^{-6}$ mole cm^{-3} and $l=2\times10^{-2}$ cm), and assuming that the smallest measurable current is $i_{SS}=10^{-6}$ A, the smallest rate constant which can be determined by this method is 0.5×10^{-3} s^{-1}.

The rates of slow reaction can be studied also by a different method: the method of current decay in the pseudo-stationary state. The electrode potentials of a thin-layer cell are fixed on either side of the equilibrium potential of the redox couple (R–O) in order to establish a limiting steady-state current proportional to the concentration of R.

If the concentration of Z is constant, the current i_{SS} will fall according to the law which describes the rate of

a reaction of the m-th order. Hence, for $m = 1$, the function $i_{SS} = f(t)$ should be of the form

$$\ln \frac{(i_d)_{ss}}{nFAD_R} = -\frac{k(Z)^p t}{(D_R/D_O + 1)} . \quad (68)$$

The upper limit of reaction rate which can be measured by this method is the same as for the previous method. However, there is no lower limit in this case because the steady-state current can be monitored as long as necessary.

Steady-state currents can be used also to measure the rate constants of fast and intermediate bimolecular reactions of the type

$$\begin{aligned} &A + ne \rightarrow B && x = 0 \\ &C \rightarrow D + ne && x = l \\ &B + D \xrightarrow{k} A + C && 0 < x < l . \end{aligned}$$

Measurements of the steady-state current i_{SS} as a function of time offer the possibility of continuous control of chemical reactions leading to changes in the concentration of O and R in the thin layer.

This approach has been used to measure the rate constants of a number of reactions [44,45]. McDuffie and coworkers [44] applied the principle in their work on the rate of the benzidine rearrangement, which occurs by the mechanism

$$O \underset{-ne}{\overset{+ne}{\rightleftharpoons}} R \xrightarrow{k} P .$$

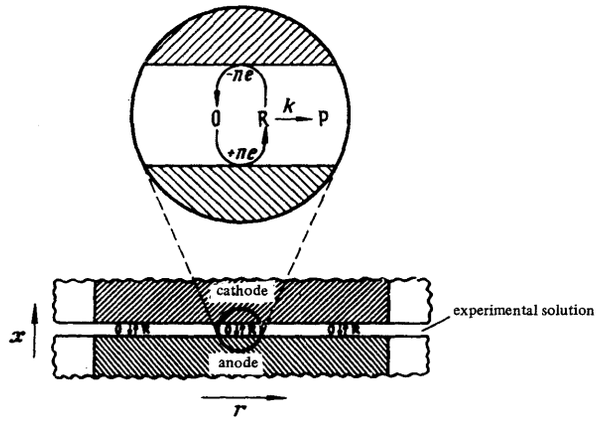


Figure 15. Cross-section of a thin-layer cell with paired electrodes.

A solution of azobenzene of known acidity, ionic strength, and ethanol concentration is added to the thin-layer cell. In order to obtain the limiting steady-state current, the electrode potentials are set so that the concentrations of O and R at the appropriate surface are both zero (Fig. 15). This current falls off exponentially with time, because the species R is consumed in the pseudo-first order irreversible rearrangement. The steady-state current is related to the concentrations of electrically active substances by the expression

$$i_{ss} = \frac{2nFAc}{l}\left(\frac{D_O D_R}{D_O + D_R}\right) \quad (69)$$

where $c = cO + cR$.

The mutual interconversion of O and R takes place at opposite electrodes. It is assumed that mass transfer is much faster than the chemical rearrangement, i.e. $(D/l^2) \gg k$, where $D = DO + DR$.

Under these conditions the distribution of O and R between the electrodes is effectively linear. The rate of a pseudo-first order chemical reaction is

$$\frac{dc_P}{dt} = \frac{dc}{dt} = kc_P . \quad (70)$$

Since the flows to the two electrodes are equal under quasi-steady state conditions, $DOcO = DRcR$. Hence, cR, which is equal to $(c - cO)$, can be expressed as

$$c_R = \frac{c}{1 + D_R/D_O} . \quad (71)$$

Inserting this expression into Eqn. (70), and integrating, we obtain

$$\ln\left(\frac{c}{c^0}\right) = -\frac{kt}{1 + D_R/D_O} \quad (72)$$

where c^0 is the total concentration of O and R at time $t = 0$. Replacing concentrations by currents (see Eqn. (69)) we obtain an expression for the decrease in current:

$$\ln(i_{ss}/i_{ss}^0) = -\frac{kt}{1 + D_R/D_O} . \quad (73)$$

The rate constant for the decay of the steady-state current is

$$k/(1 + D_R/D_O) .$$

If $D_R = D_O$, the rate constant for the current decay is $k/2$, and the plot of $\lg i_{SS}$ against t is a straight line of slope $-k/4.606$ for a pseudo-first order reaction.

Thus, the measurement of rate constants from the decay of the steady-state current i_{SS} is independent of the parameters of the thin-layer cell and of the initial concentration of the material. The experimental values of the rate constant for the acid-catalysed benzidine rearrangement, using the steady-state current decay method, are 0.113 s^{-1} in 0.25 M $HClO_4$, 0.0422 s^{-1} in 0.15 M $HClO_4$, 0.0223 s^{-1} in 0.1 M $HClO_4$, and 9.0×10^{-3} s^{-1} in 0.063 M $HClO_4$. These values are in good agreement with measurements [18] of k for the benzidine rearrangement by the thin-layer potentiostatic method (0.02 s^{-1} in 0.0997 M $HClO_4$ and 0.0086 s^{-1} in 0.063 M $HClO_4$).

The steady-state current decay method can be used also to measure the rate constants of second-order reactions. As an example, McDuffie and Reilley [45] consider the disproportionation of quinquevalent uranium in perchloric acid:

$$O \underset{}{\overset{e}{\rightleftharpoons}} R$$
$$2R \longrightarrow aO + (2 - a)Z$$

Another possible example is dimerisation, when O is not regenerated. These second-order systems are difficult to investigate by the usual electrochemical methods [46-49] because of the need to use non-linear differential equations, for which analytical solutions are not available, in the interpretation of the results.

III. SPECIAL FEATURES AND SCOPE OF THIN-LAYER ELECTROCHEMISTRY

1. Edge Effect

One of the special features of thin-layer electrochemistry is the presence of an edge effect, i.e. the effect of diffusion of electrically active substances from the bulk of the solution into the narrow gap between the working electrodes or between the working electrode and the inert substrate. The edge effect is responsible for an appreciable fraction of the residual current in the thin-layer cell. The error introduced by the edge effect into the observed steady-state current is proportional to the total excess number of moles of O and R (N_{exc}) in the thin layer of solution at time t.

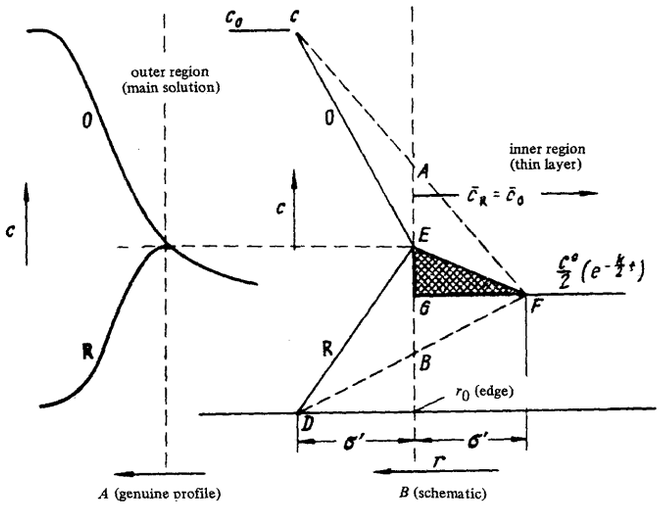


Figure 16. Schematic representation of the concentration profiles of O and R in the thin layer, used in the definition of the edge effect.

The quantity N_{exc} depends on the combined rates of diffusion of both forms of the material from the main bulk of the solution through the cylindrical edge of the thin layer. This rate of diffusion, in turn, depends on the concentration gradients of the electrically active species in the thin-layer region. It is very difficult to allow for all these conditions in a calculation of the contribution of the edge effect to the observed steady-state current. However, an approximate calculation can be made using a simplified model[44]. Immediately after the application of the potential difference ΔE the average concentration of the two forms in the thin layer is $c^0/2$, and there is no nett flow of material into the thin layer. After time t the concentration profile in the region of the edge of a thin-layer element of volume (of radius r_0) can be assumed to be of the type shown in Fig. 16. The concentration distribution is plotted for a point on the x-axis at $l/2$. In the central region of the thin-layer volume ($r/2$) the concentrations of R and O show an exponential decrease which is not distorted by the edge effect. In the schematic diagram the excess of material (N_{exc}) is found mainly in the concentration region within the triangle EGF, which penetrates from the edge into the thin layer to a depth σ^1. The region of excess concentration has the volume $\pi l[r_0^2 - (r_0 - \sigma^1)^2]$ or $\pi l\sigma^1 - (2r_0 - \sigma^1)$. The total excess of O and R, c_{exc}, can be expressed

$$c_{exc} = (c_{edge} - c_{centre})/2 \qquad (74)$$

where c_{edge} and c_{centre} denote the mean combined concentrations (O + R) at $r = r_0$ and $r = 0$ respectively. Point E is taken half-way between points A and B, and from the condition that c_{edge} can be obtained by doubling c_R or c_O at the point E we find

$$c_{edge} = (c^0 + c_{centre})/2 \, . \qquad (75)$$

Using the expression

$$c_{centre} = c^0 e^{-(k/2)t},$$

we obtain

$$c_{exc} = \frac{c^0}{4}[1 - e^{-(k/2)t}] \, . \qquad (76)$$

Multiplying Eqn. (76) by the volume,

$$N_{exc} = \frac{c^0}{4}[1 - e^{-(k/2)t}]\pi l\sigma'(2r_0 - \sigma') \qquad (77)$$

and after dividing by $N^0 = c^0\pi l r_0^2$ we arrive at

$$\frac{N_{exc}}{N^0} = [1 - e^{-(k/2)t}]\left(\frac{\sigma'}{2r_0}\right)\left(1 - \frac{\sigma'}{2r_0}\right). \qquad (78)$$

Since the limiting steady-state current is proportional to the number of moles in the thin layer of solution[43], and since σ' is approximately equal to $2(Dt/\pi)^{1/2}$, we finally obtain the equation for the relative error in the current:

$$\frac{i_{ss\ (error)}}{i^0_{ss}} = \left\{[1 - e^{-(k/2)t}]\left(\frac{Dt}{\pi r_0^2}\right)^{1/2}\left[1 - \left(\frac{Dt}{\pi r_0^2}\right)^{1/2}\right]\right\} . \qquad (79)$$

The edge effect can be minimised by increasing the radius of the working electrode. However, errors due to lack of parallelism between the electrodes become predominant above a certain electrode size. An alternative approach is to fit a plastic ring round the periphery of the thin layer, but in this case it becomes impossible to use an auxiliary and a standard electrode.

2. Influence of Lack of Parallelism and of Surface Roughness of the Working Electrode

A knowledge of the effective thickness l of the layer of solution is essential in all experiments with thin-layer electrolytic cells. The largest steady-state currents are obtained with the smallest layer thicknesses. Furthermore, the electrode separation determines the number of moles of O and R in the thin layer of solution. Both these effects can be perturbed by lack of parallelism and of smoothness in the electrode surfaces. Any roughness protruding into the layer of solution decreases the average thickness of the layer[43], and may decrease i_{ss} by a large amount. The effect of deviations from the ideal plane-parallel geometry of the electrodes can be discussed in terms of the simple model shown in Fig. 17. Using Eqn. (55) we obtain the following equation for the dependence of i_{ss} on $1/l$

$$(i_d)_{ss} = \int_0^a \frac{anFD\,(c_{R_{ss}})_{x=0}}{(l-q) + 2q/ay}\,dy = \frac{a^2nFD\,(c_{R_{ss}})}{2q}\ln\left(\frac{l+q}{l-q}\right). \qquad (80)$$

The equation has been tested, and found to be sufficiently accurate for $l \ll 4q$.

When $l = 4q$ the value of $(id)_{ss}$ calculated by Eqn. (80) is 91% of the ideal value (calculated by Eqn. (64)). These calculations suggest that the effects arising from lack of parallelism can be reduced to an acceptable minimum.

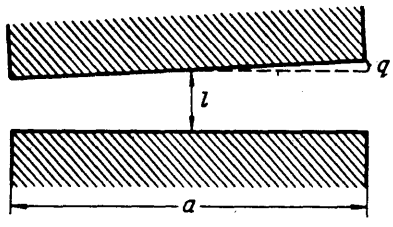


Figure 17. Lack of parallelism between the electrodes of a thin-layer electrolytic cell.

3. Scope and Advantages of the Methods of Thin-layer Electrochemistry

The main advantages of the methods of thin-layer electrochemistry were mentioned in the theoretical discussion given in the previous Sections. The most obvious attractions of thin-layer electrochemistry are the shorter analysis times and the very small volumes of solution needed.

The thin-layer electrochemical cell with a pair of working electrodes can also be used successfully when one of the reactions is hindered by the insoluble product of the other reaction. For example, if I^- and Cl^- ions are present in solution, one of the working electrodes can be used to accommodate a film of Hg_2I_2 (using mercury or an amalgam electrode), and the chloride ion is subsequently deposited on the other electrode.

Like the rotating-disk method with guard ring, the thin-layer methods are particularly useful for studies of chemical reactions preceding or following the electrode reaction, for monitoring short-lived intermediate states of the products of the electrode reaction, and for studying adsorption on the electrode surface.

Thin-layer methods show special promise in the study of adsorption processes, because they offer the possibility of working with such small volumes and concentrations that the total number of moles contained in the interelectrode gap need not be greater than the amount of material adsorbed on the electrode surface.

Thin-layer electrochemistry offers a convenient method of measuring the number n of electrons which take part in the electrode reaction, because the diffusion coefficient need not be known if n is measured by thin-layer chronopotentiometry.

Another potential advantage of thin-layer electrochemistry is the absence of hydrodynamic motion in the solution: as a result, the intermediate products of the reaction are not removed from the sphere of action by convection. The rate of supply of material by diffusion can be varied by varying the distance between the electrodes, and can be made very large. By using optically flat surfaces, the thickness of the diffusion layer can be made as small as 0.1 μm. [50] This is an order of magnitude less than the thickness of the diffusion layer for the rotating electrode (for $D = 10^{-5}$ cm^2 s^{-1}, and with a speed of rotation of 6000 r.p.m., the thickness of the diffusion layer can be reduced only to 5μm).

The use of thin-layer methods in studies of bimolecular reactions also deserves a mention.

When a pair of electrodes of different metals is used, each of the electrodes can be used in the most favourable conditions. Some other advantages of the thin-layer method are mentioned by Andersen and coworkers [51].

IV. PRACTICAL APPLICATIONS OF THIN-LAYER ELECTROCHEMISTRY

In addition to their applications (already mentioned) in the measurement of the rate of chemical reactions [1,16,20,42-45], the study of adsorption processes [3,22-24], the study of irreversibility in electrode reactions [8,24,34,43], the determination of the number of electrons involved in reactions in aqueous and non-aqueous media [2,4,40] and of diffusion coefficients [13,43,44], thin-layer methods can be used to enhance the sensitivity of analytical methods by dissolving weighed amounts of solute in very small volumes of solvent [7,9,52].

Using the equation for the limiting steady-state current $(id)_{ss}$

$$\frac{N}{lA} = \frac{(i_d)_{ss} l}{2nFA}\left(\frac{1}{D_R} + \frac{1}{D_O}\right) \qquad (81)$$

where N is the total number of moles of the oxidised and the reduced form, we can readily calculate the lower concentration limit for a one-electron reaction.

It can be seen from Eqn. (81) that $(id)_{ss}$ is proportional to the total number of moles in the thin layer and inversely proportional to the distance between the electrodes. If the steady-state current is set at 1 μA, and $l = 10^{-3}$ cm, we find that $N/lA = 10^{-9}$ mole cm^{-3} for $D_R = D_O$ (usually $\sim 10^{-5}$ cm^2 s^{-1}).

Thin-layer cells can be used also in combined electrochemical and spectral studies, which offer a powerful means of investigating the nature of electrolysis products [10,11,53].

REFERENCES

1. L. B. Andersen and C. N. Reilley, J. Electroanalyt. Chem., 10, 538 (1965).
2. C. R. Christensen and F. C. Anson, Analyt. Chem., 35, 205 (1963).
3. A. T. Hubbard and F. C. Anson, J. Electroanalyt. Chem., 9, 163 (1965).
4. J. E. McClure and D. L. Maricle, Analyt. Chem., 39, 236 (1967).
5. J. C. Sheaffer and D. G. Peters, Analyt. Chem., 42, 430 (1970).
6. A. T. Hubbard and F. C. Anson, Analyt. Chem., 36, 723 (1964).
7. Y. S. Lyalikov and R. S. Tyurin, Zhur. Anal. Khim., 24, 186 (1969).
8. A. T. Hubbard and F. C. Anson, Analyt. Chem., 40, 615 (1968).
9. R. S. Tyurin and L. G. Madan, Izv. Akad. Nauk Mold-SSR, 3, 66 (1970).
10. W. R. Heineman, J. N. Burnett, and R. W. Murray, Analyt. Chem., 40, 1970 (1968).
11. W. R. Heineman, J. N. Barnet, and R. W. Murray, Analyt. Chem., 40, 1974 (1968).

12. G. Arken, "Matematicheskie Metody v Fizike" (Mathematical Methods in Physics), Atomizdat, Moscow, 1970, p. 600.
13. T. Kuwana and R. N. Adams, J. Amer. Chem. Soc., 79, 3609 (1957).
14. K. Vetter, "Elektrochemische Kinetik" (Translated into Russian), Izd. Khimiya, Moscow, 1967.
15. D. M. Oglesby, S. H. Omang, and C. N. Reilley, Analyt. Chem., 37, 1312 (1965).
16. C. R. Christensen and F. C. Anson, Analyt. Chem., 36, 495 (1964).
17. E. Knobloch, Coll. Czech. Chem. Comm., 14, 508 (1949).
18. W. K. Snead and A. E. Remick, J. Amer. Chem. Soc., 79, 6121 (1957).
19. A. C. Testa and W. N. Reinmuth, Analyt. Chem., 32, 1512 (1960).
20. D. M. Oglesby, J. D. Johnson, and C. N. Reilley, Analyt. Chem., 38, 385 (1969).
21. W. T. DeVries and E. Van Delen, J. Electroanalyt. Chem., 8, 366 (1964).
22. R. A. Osteryoung and F. C. Anson, Analyt. Chem., 36, 975 (1964).
23. A. T. Hubbard, R. A. Osteryoung, and F. C. Anson, Analyt. Chem., 38, 692 (1966).
24. A. T. Hubbard and F. C. Anson, Analyt. Chem., 38, 1601 (1966).
25. I. N. Newson and A. C. Reddiford, J. Electrochem. Soc., 108, 699 (1961).
26. S. Schuldiner and C. H. Presby, J. Electrochem. Soc., 111, 457 (1964).
27. N. A. Balashova, Zhur. Fiz. Khim., 32, 2266 (1958).
28. N. A. Balashova, Z. phys. Chem., 207, 340 (1957).
29. N. A. Balashova and N. S. Merkulova, "Trudy Chetvertogo Soveshchaniya po Elektrokhimii" (Proceedings of the Fourth Electrochemical Conference), Izd. Akad. Nauk SSSR, Moscow, 1959, p. 48.
30. A. N. Frumkin, "Transactions of the Symposium on Electrode Processes" (E. Yaeger, Editor), New York, 1959, p. 1.
31. V. E. Kazarinov and N. A. Balashova, Dokl. Akad. Nauk SSSR, 134, 864 (1960).
32. A. D. Obrucheva, Zhur. Fiz. Khim., 32, 2155 (1958).
33. A. D. Obrucheva, Dokl. Akad. Nauk SSSR, 141, 1413 (1961); 142, 859 (1962).
34. A. T. Hubbard and F. C. Anson, Analyt. Chem., 38, 58 (1966).
35. J. E. B. Randles, Trans. Faraday Soc., 44, 3241 (1950).
36. A. Ševčik, Coll. Czech. Chem. Comm., 13, 349 (1948).
37. A. T. Hubbard, J. Electroanalyt. Chem., 22, 165 (1969).
38. F. C. Anson, Analyt. Chem., 36, 520 (1964).
39. F. C. Anson, J. Electrochem. Soc., 110, 436 (1963).
40. A. T. Hubbard and F. C. Anson, Analyt. Chem., 38, 1887 (1966).
41. W. R. Mason and R. C. Johnson, J. Electroanalyt. Chem., 4, 345 (1967).
42. J. P. Cushing and A. T. Hubbard, J. Electroanalyt. Chem., 23, 183 (1969).
43. L. B. Andersen and C. N. Reilley, J. Electroanalyt. Chem., 10, 295 (1965).
44. B. McDuffie, L. B. Andersen, and C. N. Reilley, Analyt. Chem., 38, 883 (1966).
45. B. McDuffie and C. N. Reilley, Analyt. Chem., 38, 1881 (1966).
46. G. L. Booman and D. T. Pence, Analyt. Chem., 37, 1366 (1965).
47. S. W. Feldberg and C. Auerbach, Analyt. Chem., 36, 505 (1964).
48. O. Fisher and O. Dračka, Coll. Czech. Chem. Comm., 24, 3046 (1959).
49. J. Koryta and J. Koutecky, Coll. Czech. Chem. Comm., 20, 423 (1955).
50. H. Dahms, J. Electroanalyt. Chem., 11, 62 (1966).
51. L. B. Andersen, B. McDuffie, and C. N. Reilley, J. Electroanalyt. Chem., 12, 477 (1966).
52. R. S. Tyurin, "Materialy Pyatoi Konferentsii Molodykh Uchenykh Moldavii" (Transactions of the Fifth Conference of Young Moldavian Scientists), 1967.
53. A. Yildiz, P. T. Kissinger, and C. N. Reilley, Analyt. Chem., 40, 1018 (1968).

Institute of Chemistry of the
MoldSSR Academy of Sciences,
Kishinev

Institute of Electrochemistry
of the USSR Academy of
Sciences, Moscow